ACS Sustainable Chemistry & Engineering

Research Article

Cite This: ACS Sustainable Chem. Eng. 2019, 7, 13941−13948

pubs.acs.org/journal/ascecg

A Microporous Organic Copolymer for Selective CO_2 Capture under Humid Conditions

Mahmoud M. Abdelnaby,[†,‡] Naef A. A. Qasem,[#] Bassem A. Al-Maythalony,[#] Kyle E. Cordova,[‡,§] and Othman Charles S. Al Hamouz*[,†]

[†]Department of Chemistry, King Fahd University of Petroleum and Minerals (KFUPM), Dhahran 31261, Saudi Arabia

[‡]Center for Research Excellence in Nanotechnology (CENT), King Fahd University of Petroleum and Minerals (KFUPM), Dhahran, 31261, Saudi Arabia

[#]King Abdulaziz City for Science and Technology − Technology Innovation Center on Carbon Capture and Sequestration (KACST-TIC on CCS), King Fahd University of Petroleum and Minerals (KFUPM), Dhahran, 31261, Saudi Arabia

[§]Department of Chemistry and Berkeley Global Science Institute, University of California—Berkeley, Berkeley, California 94720, United States

Supporting Information

ABSTRACT: A cross-linked microporous organic copolymer, termed KFUPM-2, was synthesized through a Friedel−Crafts alkylation polymerization of phenothiazine, pyrrole, and *p*-formaldehyde in the presence of iron(III) chloride catalyst. KFUPM-2 was demonstrated to have intrinsic permanent microporosity with a Brunauer−Emmett−Teller surface area of 352 $m^2\ g^{-1}$ and a high capacity (39.1 $cm^3\ g^{-1}$ at 273 K and 760 Torr) and affinity (Q_{st} = 34 kJ mol^{-1} and CO_2/N_2 selectivity of 51) toward CO_2 as a result of its nitrogen-rich structure. To demonstrate its practical applicability, breakthrough measurements were performed using a gas mixture that mimicked the composition of an industrial flue gas stream (CO_2/N_2 = 20/80% *v*/*v* with 91% relative humidity). Accordingly, KFUPM-2 was shown to have an ultrahigh CO_2 dynamic capacity (32 $cm^3\ g^{-1}$ at 298 K) in the presence of water and was demonstrated recyclable over at least 10 cycles with mild regeneration conditions needed between each cycle.

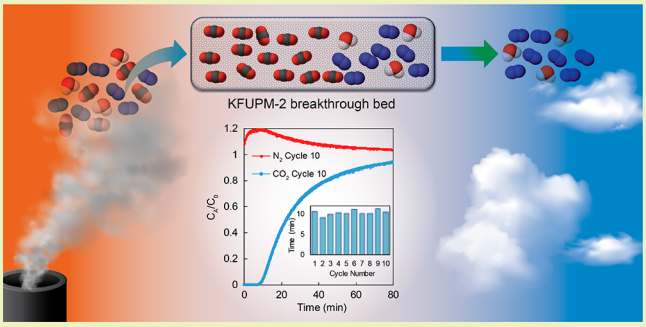

KEYWORDS: *Microporous polymers, Carbon dioxide capture, Polymer chemistry, Postcombustion flue gas, Dynamic separation*

INTRODUCTION

It is widely recognized by the international scientific community that atmospheric CO_2 levels are rising and playing a prominent role in accelerating climate change.[1] One of the single greatest anthropogenic contributors to this problem is coal- and natural gas-fired power plants.[3,4] For example, in a typical 500 MW coal-fired power plant, more than 3 million tons of CO_2 is emitted per year.[5] With a lack of widespread implementation of alternative energy sources, these contributors have caused atmospheric CO_2 levels to climb above 400 ppm for the first time in recorded history.[2] When considering the enormity of the CO_2 emission problem together with the relatively slow implementation of alternative and cleaner energy sources, the capture and sequestration (CCS) of CO_2 at point sources is of the utmost importance in the near future.[6,7] However, despite decades of investigation into potential avenues for achieving scalable, cost-effective, and energy-efficient CCS technologies, the most widely employed technique to date remains the use of aqueous monoethanolamine (MEA) solutions.[8] In this process, flue gas from power plants is passed through an MEA solution, which captures CO_2 via chemisorptive covalent bond formation (*e.g.* ammonium carbamate formation).[9] Although MEA is extremely effective at capturing CO_2 in this fashion, the overall process is not energy efficient due to the high heat capacity of the aqueous MEA solutions (25−40% of a power plant's energy output is required for regeneration), lacks long-term reusability, and carries significant capital costs to sustain the employment of this corrosive solution.[10]

Compared to aqueous MEA solutions, CCS using solid adsorbents represents an ideal route for lowering energy costs and establishing long-term reusability without loss in performance in addition to being overall more environmentally friendly.[11] For a solid adsorbent material to be considered attractive it must achieve exceptional performance under the prescribed general conditions of flue gas mixtures.[12] The general conditions for a postcombustion flue gas stream from a coal-fired power plant are close to ambient pressure (∼1 bar)

Received: April 26, 2019
Revised: July 15, 2019
Published: July 17, 2019

DOI: 10.1021/acssuschemeng.9b02334
ACS Sustainable Chem. Eng. 2019, 7, 13941−13948

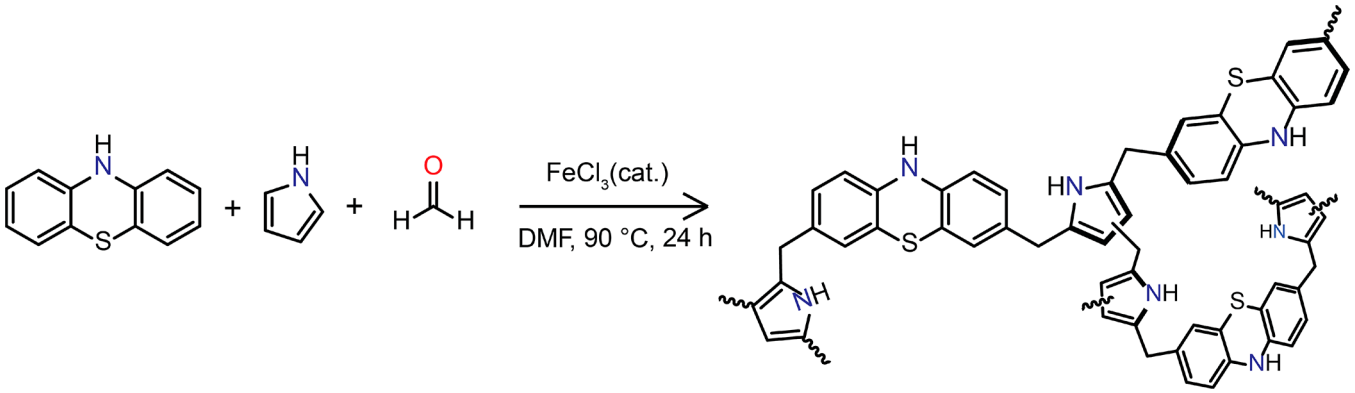

Figure 1. Synthesis of KFUPM-2. The synthesis followed a Friedel–Crafts alkylation polymerization of phenothiazine with pyrrole via *p*-formaldehyde as a cross-linking agent and ferric chloride as the Lewis acidic catalyst.

and slightly elevated temperatures (40–80 °C) with a composition of N_2 (70–75%), CO_2 (15–16%), and H_2O (5–7%), among other lesser gaseous components, by volume.[13,14] The challenge, therefore, lies not in the operational conditions (i.e., pressure and temperature), but rather in the selectivity of the prospective solid sorbent for CO_2 in the presence of other competitor gases, most notably N_2 and H_2O. Traditional solid adsorbents, including porous carbon, zeolites, and metal–organic frameworks, have contributed significantly to our understanding of the structure–property relationship needed for this application.[15−21] From this foundation, a class of materials, known as porous organic polymers, have emerged as prominent candidates due to their ease of synthesis, exceptional chemical stability, outstanding physicochemical properties, immense structural diversity with potential for chemical modification, and high internal surface areas.[22,23] A wide range of porous organic polymers, such as covalent organic frameworks (COFs),[24,25] crystalline triazine frameworks (CTFs),[26,27] porous aromatic frameworks (PAFs),[28] hypercross-linked polymers (HCPs),[29−31] and conjugated microporous polymers (CMPs),[32] have proven their potential to be exploited for CO_2 capture. Combined experimental and simulation studies have shown that incorporating phenyl rings and polar functionalities enhance the binding affinity to CO_2,[33] improving the surface area leads to higher uptake,[26−28,33] and tuning the pore size has the potential to impact selectivity. Nevertheless, there have been few reports in which a porous organic polymer was demonstrated feasible for selectively capturing CO_2 under practical conditions.[31,34−38]

Herein, we report the synthesis and structural characterization of a new microporous organic copolymer, termed KFUPM-2. The synthesis strategy for realizing KFUPM-2 was based on a one-pot Friedel–Crafts alkylation polymerization of inexpensive monomers, phenothiazine, and pyrrole, which were cross-linked by *p*-formaldehyde in the presences of a catalytic amount of iron(III) chloride (Figure 1). The resulting polymer was proven permanently microporous and, as a result of its nitrogen-rich backbone, was demonstrated capable of adsorbing CO_2 through strong physisorptive interactions. Furthermore, KFUPM-2 was shown to selectively adsorb CO_2 under humid conditions (32 $cm^3\ g^{-1}$ at 91% relative humidity) and was capable of being regenerated with no energy input without loss of performance over 10 cycles. This report highlights a new porous organic polymer material that is among the best performing solid adsorbents for carbon capture under practical, industrially relevant conditions.

EXPERIMENTAL SECTION

Materials and General Procedures. Full synthetic and characterization details can be found in the Supporting Information, sections S1 and S2. Pyrrole (98% purity), methanol (99.9% purity), and *N*,*N*′-dimethylformamide (99% purity) were purchased from Sigma-Aldrich Co. Anhydrous iron(III) chloride (≥99.99% purity) was obtained from Alpha Chemika. Phenothiazine (98% purity) and *p*-formaldehyde (≥99% purity) were purchased from Fluka. Pyrrole was distilled under N_2 flow at 145 °C prior to use. All other chemicals were used without further purification. For gas sorption measurements, ultrahigh purity grade nitrogen (99.999%), helium (99.999%), and high purity CO_2 (99.9%) were obtained from Abdullah Hashem Industrial Co., Dammam, Saudi Arabia. Solid state ^{13}C nuclear magnetic resonance (NMR) spectroscopy measurements were carried out on a Bruker 400 MHz spectrometer operating at 125.65 MHz (11.74 T) and at ambient temperature (298 K). Samples were packed into 4 mm ZrO_2 rotors and cross-polarization magic angle spinning (CP-MAS) was employed with a magic angle spinning rate of 14 kHz. Fourier transform infrared (FT-IR) spectroscopy measurements were performed on a PerkinElmer 16 PC spectrometer using KBr pellets. The spectra were recorded over 4000–600 cm^{-1} in transmission mode, and the output signals were described as follows: s, strong; m, medium; w, weak; and br, broad. CHN analysis was carried out on a PerkinElmer (EA-2400) elemental analyzer. Thermogravimetric analysis (TGA) was run on a TA Q-500 instrument with a platinum pan sample holder. For this measurement, ∼10 mg of sample was heated under air flow with a heating rate of 10 °C min^{-1}. Powder X-ray diffraction (PXRD) measurements were recorded on a Rigaku MiniFlex II X-ray diffractometer with Cu Kα radiation (λ = 1.54178 Å). Low pressure nitrogen sorption isotherms were performed using a Quantachrome Quadrasorb-Evo instrument. A liquid nitrogen bath was used for the measurements at 77 K. CO_2 sorption isotherms were measured on an Autosorb iQ2 volumetric gas adsorption analyzer. The measurement temperatures at 273 and 298 K were controlled with a water circulator.

Synthesis of KFUPM-2. Phenothiazine (0.40 g, 2.00 mmol) and *p*-formaldehyde (0.36 g, 12.0 mmol) were dissolved in 20 mL of DMF in a 50 mL round-bottom flask and stirred at room temperature for 5 min. Then, pyrrole (0.40 g, 6.00 mmol) was added, and the reaction mixture was stirred for an additional 5 min and purged with N_2 for 2–3 min. At this time, ferric chloride ($FeCl_3$, 0.194 g, 1.20 mmol) was added under inert atmosphere, and the flask was sealed with a rubber septum. The reaction was heated by a preheated oil bath at 90 °C and continuously stirred for 24 h with a rate of 500 rpm (a black solid was formed after 10 min). The resulting solid was washed with 20 mL of methanol followed by sonication for 30 min. The solid was then rigorously washed with 30 mL of methanol two times per day for 5 days with stirring until a clear filtrate solution was obtained. Finally, the product was dried at 80 °C in an oven for 12 h. The final yield (0.87 g) was 92% based on the monomer weights (after excluding the equivalent amount of water as a byproduct). Anal. Calcd for

DOI: 10.1021/acssuschemeng.9b02334
ACS Sustainable Chem. Eng. 2019, 7, 13941−13948

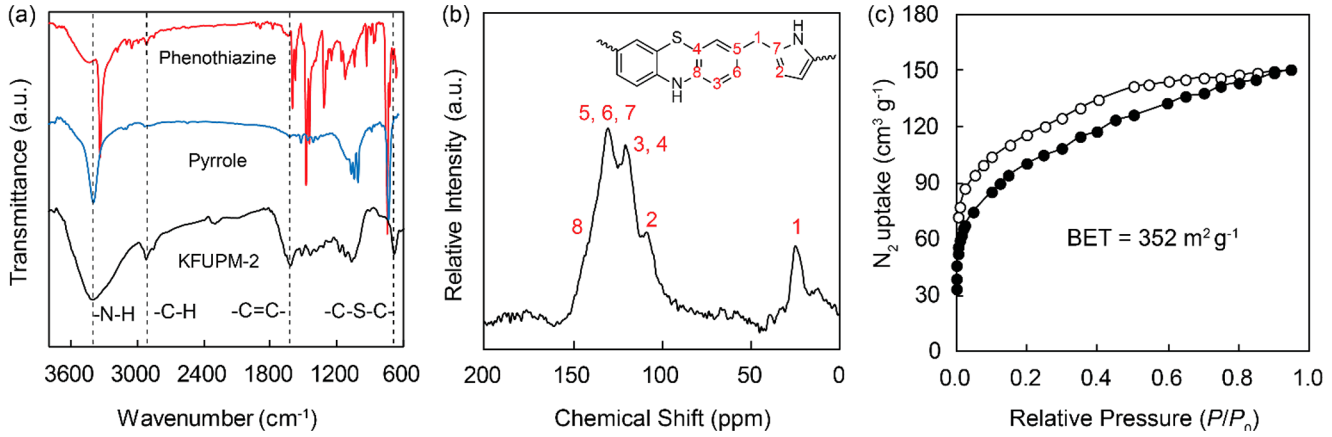

Figure 2. Structural characterization of KFUPM-2. (a) Fourier transform-infrared spectroscopy (FT-IR) spectra of KFUPM-2 (black) in comparison to pure phenothizaine (red) and pure pyrrole (blue). Those absorption bands directly related to the characteristic functionalities of KFUPM-2 are highlighted. (b) Cross-polarization-magic angle spinning solid state nuclear magnetic resonance (CP-MAS ^{13}C NMR) spectrum at 14 kHz with the corresponding peak assignments. Inset: The core structure of KFUPM-2 is provided for peak assignment. (c) N_2 isotherms measured at 77 K. Filled and open circles correspond to the adsorption and desorption curves, respectively.

$C_{29}H_{26}N_4S$: C, 75.29, H 5.66, N 12.11, S 6.93. Found C, 51.47, H 3.24, N 10.07, S 1.79. FT-IR (KBr, cm^{-1}): 3430 (br), 2920 (w), 2860 (w), 1620 (w), 1410 (w), 1020 (w), and 747 (w).

Breakthrough Measurements. Full details regarding the breakthrough setup used for this study and the measurement parameters are provided in the Supporting Information, section S5. In a typical measurement, a fixed bed was packed with KFUPM-2 powder (0.63 g), and the sample was activated at 373 K for 24 h under vacuum prior to carrying out the measurement. The breakthrough experiments were conducted under ambient conditions (298 K and 1 bar) with a 10 sccm flow rate of CO_2:N_2(20:80 *v*/*v*) feed mixture. For the measurements under humid conditions, a dry N_2 gas stream was passed through a water humidifier at room temperature, which was then passed through the sample bed. The water level in the gas stream was monitored by mass spectrometry until saturation was obtained (91% RH). The full dynamic capacity of CO_2 and N_2 was estimated by evaluating the ratio of compositions of the downstream gas and the feed gas. The regeneration of the sample was conducted at room temperature by flow of pure wet N_2 through the sample bed for 5−6 h.

RESULTS AND DISCUSSION

Synthesis Strategy. The synthetic approach for synthesizing a new, CO_2-philic, microporous polymer relied on a modified Friedel−Crafts alkylation polymerization.[29] Phenothiazine and pyrrole were chosen as monomers due to their polar structures—an important consideration for increasing the affinity of CO_2 to the backbone of the resulting polymer. For the polymerization reaction, phenothiazine and pyrrole were dissolved in *N*,*N*′-dimethylformamide (DMF) in a molar ratio of 1:3. The molar ratio of these monomers was initially varied, and ultimately, it was found that the 1:3 ratio was optimal for producing the polymer with the highest surface area. DMF was chosen due to its high boiling point (153 °C) and its solvation ability, both of which proved important for this polymerization. An excess of cross-linking agent, *p*-formaldehyde, was also added together with $FeCl_3$ catalyst (chosen for its strong Lewis acidity). The reaction mixture was stirred and heated to 90 °C under an inert atmosphere for 24 h. It is noted that the polymerization occurred very rapidly with a black, insoluble solid precipitating within 10 min; however, we found that allowing the reaction to proceed for a longer period of time led to consistently higher yields and higher resulting surface areas, presumably due to increasing the degree of cross-linking within the polymer. After 24 h, the resulting polymer, termed KFUPM-2, was obtained in a 92% yield (Figure 1). To ensure reproducibility, the synthesis of KFUPM-2 was repeated over four separate batches, in which case, each batch produced the same yield, surface area, and CO_2 uptake capacity. The formation of KFUPM-2 occurs via the following proposed mechanism: *p*-formaldehyde is first activated by the $FeCl_3$ catalyst, which, in turn, leads to an electrophilic aromatic substitution with the α-carbon of a pyrrole monomer. This forms primary alcohol that serves as the precursor to the eventual methylene cross-linking unit. Upon activation, the primary alcohol leaves to yield the resonance-stabilized 1-azafulvene intermediate.[39] Through a second electrophilic aromatic substitution process, the intermediate is added to a phenothiazine monomer at the γ-carbon closest to sulfur (this is due to the electron-donating nature of the nitrogen atom in phenothiazine). Indeed, this step is critical in that the two monomers are now cross-linked together. The overall addition−elimination reaction then proceeds until all of the monomers are essentially consumed.

Structural Characterization. Given the fact that KFUPM-2 was X-ray amorphous, structural elucidation was carried out by combining Fourier transform infrared spectroscopy (FT-IR), cross-polarization magic angle spinning solid-state ^{13}C nuclear magnetic resonance spectroscopy (CP-MAS ^{13}C NMR), and thermal gravimetric analysis (TGA). The presence of both the phenothiazine and pyrrole monomers cross-linked by a methylene unit was first confirmed by FT-IR (Figure 2a). For this, an absorption band centered at 2918 cm^{-1} was identified as the −CH stretch specific for the methylene cross-linking unit between pyrrole and phenothiazine. A broad absorption band at 3413 cm^{-1} was attributed to characteristic −NH− stretching vibrations from both pyrrole and phenothiazine. Finally, the −C−S−C− absorption band was observed at 670 cm^{-1}, which again supports the presence of the phenothiazine monomer within the structure. Further direct structural support was provided by CP-MAS ^{13}C NMR spectroscopy (Figure 2b). A characteristic peak for the methylene cross-linking unit ($-CH_2$) was found at 25 ppm. It was expected that at least three distinct chemical shifts for the methylene unit would be observed due to differing electronic effects between cross-linking pyrrole−phenothia-

DOI: 10.1021/acssuschemeng.9b02334
ACS Sustainable Chem. Eng. 2019, 7, 13941−13948

zine, pyrrole−pyrrole, and phenothiazine−phenothiazine. However, we observed one broad chemical shift at 25 ppm that encompassed all of these possibilities.[40] Support for the incorporation of pyrrole was provided by a characteristic broad peak at 108 ppm—a chemical shift that was assigned to the aromatic sp^2-hybridized β-carbon atoms of this monomer. The aromatic α-carbon atoms in pyrrole (adjacent to the nitrogen atom) clearly resonate at 130 ppm. Characteristic chemical shifts for the phenothiazine monomer appeared at 120 and 140 ppm, which were assigned to the aromatic carbon atoms in this monomer. Taken together, the FT-IR and CP-MAS ^{13}C NMR provided strong evidence and support for the structure of KFUPM-2. Finally, the TGA of KFUPM-2 demonstrates this material's exceptional thermal stability up to ∼500 °C—a result that is due to a high degree of cross-linking between the monomers (Supporting Information, Figure S4). It is noted that there was no Fe_2O_3 residue remaining after completion of the TGA measurement, which is direct evidence for the absence of any trapped $FeCl_3$ catalyst within the pores.

The porosity of KFUPM-2 was assessed by N_2 adsorption measurements at 77 K (Figure 2c). In the isotherm, a sharp uptake at low relative pressure (P/P_0 < 0.001) was observed indicating KFUPM-2 is predominantly microporous in nature (i.e., Type-I profile). Hysteresis was noted upon desorption, which was attributed to the elastic deformation or swelling of the polymeric network.[41] The Brunauer−Emmett−Teller (BET) surface area of KFUPM-2, calculated at P/P_0 = 0.01−0.3, was 352 $m^2\ g^{-1}$. The pore volume, calculated using a DFT model, was 0.21 $cm^3\ g^{-1}$. Finally, by application of a quenched solid-state density functional theory model, the pore size distribution (PSD) was obtained. As expected, the PSD exhibited pore sizes primarily in the microporous size regime.

Gas Adsorption Properties. Our strategy for evaluating KFUPM-2 for use in postcombustion CO_2 capture centered on understanding four key properties: (i) thermodynamic CO_2 uptake capacity; (ii) coverage-dependent enthalpy of adsorption to understand the material's affinity toward CO_2; (iii) selectivity of KFUPM-2 toward CO_2 over N_2; and (iv) dynamic adsorption capacity, via breakthrough measurements, under both dry and wet conditions.

Thermodynamic Uptake Capacity. It is well understood through previous reports, that the ability of a material to capture CO_2 effectively depends not only on the surface area or pore nature but also the internal pore environment through its density of polarizable sites.[42] Thus, the combination of advantageous properties found in KFUPM-2 (e.g., intrinsic microporosity and nitrogen-enriched backbone) provided justification for testing this material's CO_2 adsorption properties. Accordingly, thermodynamic CO_2 adsorption isotherms were measured at 273 and 298 K (Figure 3 and Supporting Information, section S4). As is shown, the isotherms were reversible yet exhibited a small hysteresis upon desorption. This hysteresis is indicative of a strong interaction between KFUPM-2 and CO_2. Nevertheless, KFUPM-2 exhibited an overall high CO_2 uptake capacity of 39.1 $cm^3\ g^{-1}$ at 273 K and 760 Torr and 23.3 $cm^3\ g^{-1}$ at 298 K and 760 Torr. For comparison, the N_2 adsorption isotherms for KFUPM-2 showed low uptake capacities as expected (5.1 and 1.0 $cm^3\ g^{-1}$ at 760 Torr and 273 and 298 K, respectively). Upon analysis of the initial slopes of both the CO_2 and N_2 isotherms—a useful qualitative assessment of the material's interactions with the appropriate gas molecule—it is clearly evident that the slope for CO_2 adsorption is much steeper than

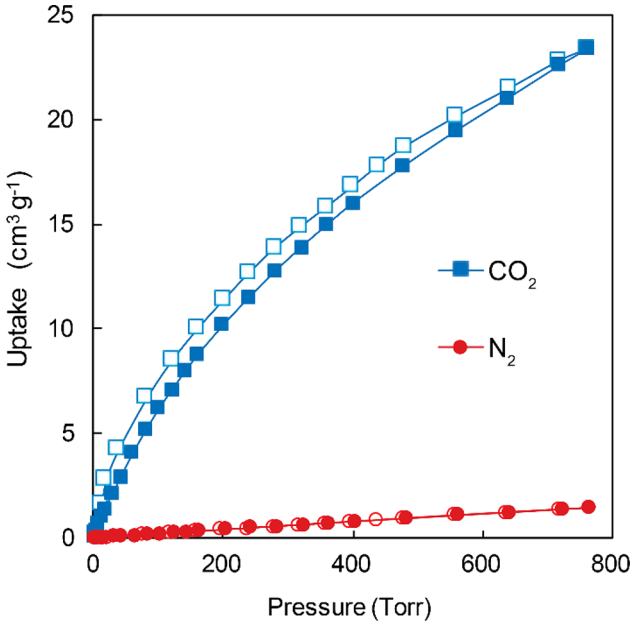

Figure 3. CO_2 (blue squares) and N_2 (red circles) adsorption isotherms for KFUPM-2 at 298 K. Filled and open symbols represent adsorption and desorption branches, respectively. The connecting lines serve as a guide to the eye.

N_2, which reflects the fact that KFUPM-2 interacts more strongly with CO_2 as opposed to N_2. The CO_2 uptake capacity of KFUPM-2 at 273 K is comparable to or higher than those capacities reported for crystalline covalent organic frameworks (COFs; COF-1:51.9 $cm^3\ g^{-1}$, COF-5:29.9 $cm^3\ g^{-1}$, COF-8:32.0 $cm^3\ g^{-1}$, and COF-10:27.0 $cm^3\ g^{-1}$).[24,43-46] Furthermore, the CO_2 uptake capacity measured for KFUPM-2 is comparable with other porous organic polymers based on similar monomers at 760 Torr and 273 K. These include: NUT-1 (36.8 $cm^3\ g^{-1}$),[47] CMP-1 (29.6 $cm^3\ g^{-1}$),[48] and PPN-6-CH_2Cl (28.6 $cm^3\ g^{-1}$) (Table 1).[49]

Coverage-Dependent Enthalpy of Adsorption and CO_2/N_2 Selectivity. With the thermodynamic uptake capacities in hand, we were encouraged to further pursue and understand the relationship of KFUPM-2 with CO_2. Accordingly, a virial-type expansion equation was employed to fit the CO_2 isotherms at 273 and 298 K in order to estimate the coverage-dependent enthalpy of adsorption (Q_{st}) (Supporting Information, section S4). The resulting initial Q_{st} value was calculated to be 34 kJ mol^{-1}, which quantifiably reflects the strong binding affinity of KFUPM-2 to CO_2. This moderately high Q_{st} value is within a favorable range for strong, yet reversible physisorption and is comparable to those for similarly related adsorbents:[23,50] BILP-1 (26.5 kJ mol^{-1}),[51] Azo-COP-1 (29.3 kJ mol^{-1}),[52] and PAF-1 (15.6 kJ mol^{-1}).[53] It is noted that as CO_2 covers the surface of KFUPM-2, the Q_{st} decreases due to the strongest binding sites being occupied. The CO_2/N_2 selectivity of the KFUPM-2 was then estimated by applying the ideal adsorption solution theory (IAST) model. As such, KFUPM-2 produces a remarkably high CO_2/N_2 selectivity (51) for a gaseous mixture containing 20% CO_2 and 80% N_2 (v/v) at pressures varying from 0 to 1 bar (Table 1).

Dynamic Breakthrough Measurements. Given the thermodynamic (static) gas adsorption properties of KFUPM-2, we sought to assess the practical capability of

DOI: 10.1021/acssuschemeng.9b02334
ACS Sustainable Chem. Eng. 2019, 7, 13941−13948

Table 1. Dynamic CO_2 Capture Properties under Wet Conditions for KFUPM-2 in Comparison with Similarly Related High-Performing Adsorbents

material	SA_{BET} (m^2 g^{-1})	CO_2 uptake (cm^3 g^{-1})[a]	CO_2/N_2 selectivity[b]	dynamic CO_2 uptake capacity (cm^3 g^{-1})[c] dry	dynamic CO_2 uptake capacity (cm^3 g^{-1})[c] wet	regeneration temp (K)	ref
KFUPM-2	352	23.3	51	9.7	32.2	298	this work
Py-1	437	42[d]	117[e]	—	—	—	29
KFUPM-1	305	23.4	141	8.5	15.1	298	31
carbon monolith (HCM-DAH-1)	670	58.2	28	20.9	20.3	298	39
Azo-COP-1	635	32	96	—	—	298	52
CTF-FUM-350	230	57.2	102	11.4	—	—	54
CTF-DCN-500	735	38.4	37	8.3	—	—	54
BPL carbon	1210	47	—	6.0	4.2	—	55
NUT-6	1138	83.5	338	—	—	333	47
NUT-10	100[f]	40.2	159	—	—	333	58
PPN-6-SO_3NH_4	593	81	196	25.8	—	363	59
LZU-301 (COF)	654	35.6	—	4.9	8.2	373	25
[HO_2C]100%-H_2P-COF	364	76	77	16.4	—	353[g]	60
FCTF-1	662	72	31	16.1	14.2	298[g]	61
FCTCz	1845	62.9	26	—	—	—	62
Fe-POP-1	875	96.3[h]	—	—	—	—	63
TPOP-1	560	60[h]	—	—	—	—	64

[a]At 298 K and 760 Torr. [b]Calculated by ideal adsorbed solution theory at 298 K and 1 bar. [c]Calculated from dynamic breakthrough experiments. [d]Calculated at 1.13 bar. [e]Calculated at 273 K by initial slope method. [f]Calculated from CO_2 isotherms at 273 K. [g]Regenerated under vacuum. [h]Calculated at 273 K. Those properties that were not reported are identified with "—".

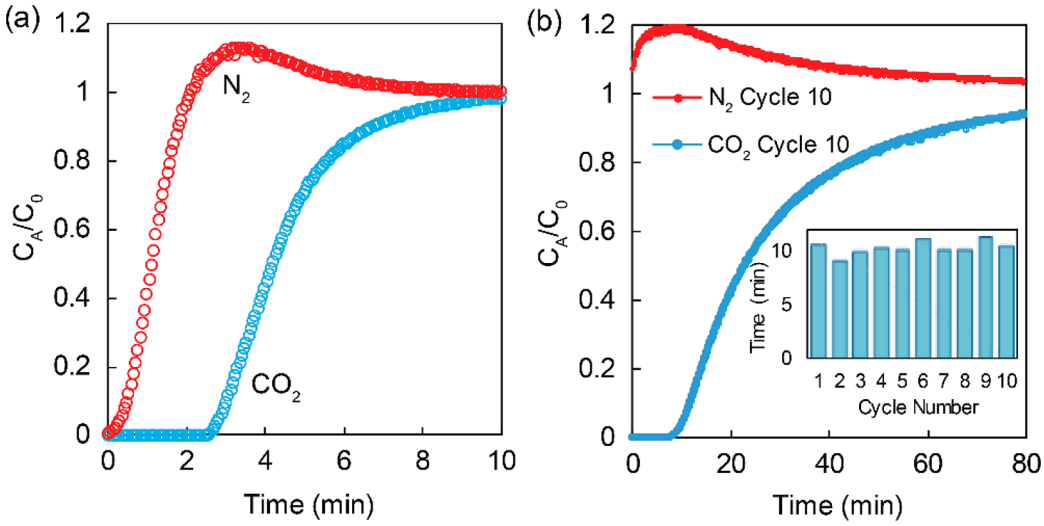

Figure 4. A 20:80 gas mixture containing CO_2 and N_2, respectively, was flown through a fixed bed of KFUPM-2 at 298 K and 1 bar (a) under dry conditions (b) under wet conditions (91% relative humidity). Inset: There is no loss in dynamic adsorption capacity over 10 consecutive breakthrough measurements.

this material for selectively capturing CO_2 from N_2 under both dry and wet conditions in a dynamic environment. The gold standard for assessing this is through a dynamic breakthrough measurement, in which an adsorbent material is exposed to a gaseous mixture and the effluent is monitored by mass spectrometry. As such, an activated sample of KFUPM-2 was subjected to a dry gaseous mixture containing 20% CO_2 and 80% N_2 (v/v)—a composition that closely resembles that found in a flue gas mixture. As shown in Figure 4a, the experimental breakthrough curves clearly demonstrate that CO_2 was retained within KFUPM-2 while N_2 passed through unencumbered. The calculated dynamic uptake capacity of CO_2, based on the breakthrough time, was 9.7 cm^3 g^{-1}. This capacity, under dry conditions, was comparable to other porous polymers, such as CTF-FUM-350 (11.4 cm^3 g^{-1}) and CTF-DCN-500 (8.3 cm^3 g^{-1}),[54] yet greater than that reported for COFs (LZU-301:4.9 c cm^3 g^{-1})[25] and commercially available BPL carbon (6.0 cm^3 g^{-1}).[55]

When taking into consideration the fact that industrial flue gas contains significant amounts of moisture (5−7% v/v),[13] effective CO_2 adsorbents must demonstrate their effectiveness in mitigating the effect of water over long periods of sustained use. Accordingly, we performed a multicycle (10 cycles total), continuous breakthrough measurement under wet conditions at 298 K. In this measurement, KFUPM-2 was first subjected to a wet N_2 stream with 91% relative humidity until the bed

DOI: 10.1021/acssuschemeng.9b02334
ACS Sustainable Chem. Eng. 2019, 7, 13941−13948

was fully saturated with water. At the point of saturation, a dry CO_2 stream (20% v/v) was then added to the wet N_2 stream and the effluent was monitored for the breakthrough time. This process was then repeated for 10 cycles, through which KFUPM-2 demonstrated an exceptionally selective and sustained dynamic CO_2 uptake capacity (32 cm^3 g^{-1}) (Figure 4 and Table 1). We speculate that the enhancement in dynamic CO_2 uptake capacity under wet conditions is a result of the fact that KFUPM-2 contains both micro- and mesopores with polar functional groups lining the pores (Supporting Information, Figure S6). This combination of structural features allows the material to adsorb significant amount of water molecules. Consequentially, a higher CO_2 uptake was observed as a result of increased CO2 solubility.[56] Additionally, we speculate that the presence of water inside the pores formed a thin film that settled on the polymer surface via a network of hydrogen bonds.[57] This thin film of adsorbed water molecules then served as binding sites for CO_2, which, in turn, attracts more water molecules that bind with additional CO_2 molecules in a cooperative fashion. We note that enhancement of CO_2 uptake in the presence of water was observed in other similarly related porous organic materials with aromatic amine groups functioning through physisorption mechanisms.[25,31]

Between each cycle, KFUPM-2 was regenerated under mild conditions by simply flowing the wet N_2 stream through the material at ambient pressure and temperature. This facile regeneration process reflects the capability of KFUPM-2 for an energy-efficient pressure swing adsorption process, which is used for continuous industrial-scale flue gas purification.

CONCLUSION

In conclusion, a new cross-linked porous polymer termed KFUPM-2 was successfully synthesized from the polycondensation of phenothiazine and pyrrole with (1:3) ratio using *p*-formaldehyde as a cross-linker with a catalytic amount of ferric chloride. The KFUPM-2 polymer proven microporous with a surface area of 352 m^2 g^{-1} and a majority of micropores (1.0 nm pore width). The KFUPM-2 showed moderate CO_2 uptake of 23.3 cm^3 g^{-1} with CO_2/N_2 selectivity of 51 at 298 K. Furthermore, the KFUPM-2 material was explored for the selective dynamic CO_2 separation from dry and wet (91% humidity) N_2 flow showing a dynamic capacity of 9.7 and 32 cm^3 g^{-1}, respectively. Additionally, a multicycle continuous breakthrough experiments (10 cycles) were performed and the regeneration between each cycle was achieved at ambient condition by simple N_2 flow. Such high recyclability and energy efficient regeneration make KFUPM-2 a promising candidate as a solid sorbent for selective CO_2 capture and separation under humid condition relevant to industrial flue gas.

ASSOCIATED CONTENT

Supporting Information

The Supporting Information is available free of charge on the ACS Publications website at DOI: 10.1021/acssuschemeng.9b02334.

KFUPM-2 synthesis and characterization (including CP-MAS ^{13}C NMR, FT-IR, PXRD, TGA curves, and adsorption isotherms) and the experimental conditions for breakthrough measurements (PDF)

AUTHOR INFORMATION

Corresponding Author

*(O.C.S.A.H.) E-mail: othmanc@kfupm.edu.sa.

ORCID

Naef A. A. Qasem: 0000-0002-3641-3996

Bassem A. Al-Maythalony: 0000-0003-3104-2214

Kyle E. Cordova: 0000-0002-4988-0497

Funding

The synthesis and characterization were supported by KFUPM (Project No. IN161034) and the gas adsorption and breakthrough studies were supported by Saudi Aramco (Project No. ORCP 2390).

Notes

The authors declare no competing financial interest.

ACKNOWLEDGMENTS

We are grateful to Prof. Omar M. Yaghi (UC Berkeley Global Science Institute) for his continued support and mentorship throughout this project. We acknowledge Prof. Zain H. Yamani (CENT, KFUPM) for use of CENT facilities as well as Prof. Rached Ben-Mansour (KACST-TIC on CCS, KFUPM) for use of his breakthrough instrument.

REFERENCES

(1) Feldman, D. R.; Collins, W. D.; Gero, P. J.; Torn, M. S.; Mlawer, E. J.; Shippert, T. R. Observational determination of surface radiative forcing by CO_2 from 2000 to 2010. *Nature* **2015**, *519* (7543), 339−343.

(2) National Oceanic and Atmospheric Administration. ESRL Global.

(3) Monitoring Division - Global Greenhouse Gas Reference Network, https://www.esrl.noaa.gov/gmd/ccgg/trends/global.html. (Accessed April 6, 2019).

(4) Boot-Handford, M. E.; Abanades, J. C.; Anthony, E. J.; Blunt, M. J.; Brandani, S.; Mac Dowell, N.; Fernández, J. R.; Ferrari, M.-C.; Gross, R.; Hallett, J. P.; Haszeldine, R. S.; Heptonstall, P.; Lyngfelt, A.; Makuch, Z.; Mangano, E.; Porter, R. T. J.; Pourkashanian, M.; Rochelle, G. T.; Shah, N.; Yao, J. G.; Fennell, P. S. Carbon capture and storage update. *Energy Environ. Sci.* **2014**, *7* (1), 130−189.

(5) Medina, R.; Tarlock, A. D. Addressing Climate Change at the State and Local Level: Using Land Use Controls to Reduce Automobile Emissions. *Sustainability* **2010**, *2* (6), 1742−1764.

(6) Liu, J.; Wang, X.; Xu, T.; Shao, G. Novel negatively charged hybrids. 1. copolymers: Preparation and adsorption properties. *Sep. Purif. Technol.* **2009**, *66*, 135−142.

(7) Haszeldine, R. S. Carbon capture and storage: how green can black be? *Science* **2009**, *325* (5948), 1647−1652.

(8) Leung, D. Y. C.; Caramanna, G.; Maroto-Valer, M. M. An overview of current status of carbon dioxide capture and storage technologies. *Renewable Sustainable Energy Rev.* **2014**, *39*, 426−443.

(9) Rochelle, G. T. Amine scrubbing for CO_2 capture. *Science* **2009**, *325* (5948), 1652−1654.

(10) Lv, B.; Guo, B.; Zhou, Z.; Jing, G. Mechanisms of CO_2 capture into monoethanolamine solution with different CO_2 loading during the absorption/desorption processes. *Environ. Sci. Technol.* **2015**, *49* (17), 10728−10735.

(11) Bhown, A. S. Status and analysis of next generation post-combustion CO_2 capture technologies. *Energy Procedia* **2014**, *63*, 542−549.

(12) Wang, J. Y.; Huang, L.; Yang, R. Y.; Zhang, Z.; Wu, J. W.; Gao, Y. S.; Wang, Q.; O'Hare, D.; Zhong, Z. Y. Recent advances in solid sorbents for CO_2 capture and new development trends. *Energy Environ. Sci.* **2014**, *7* (11), 3478−3518.

(13) Sayari, A.; Belmabkhout, Y.; Serna-Guerrero, R. Flue gas treatment via CO_2 adsorption. *Chem. Eng. J.* **2011**, *171* (3), 760−774.

(14) Granite, E. J.; Pennline, H. W. Photochemical removal of mercury from flue gas. *Ind. Eng. Chem. Res.* **2002**, *41* (22), 5470−5476.
(15) Ho, M. T.; Allinson, G. W.; Wiley, D. E. Reducing the cost of CO_2 capture from flue gases using pressure swing adsorption. *Ind. Eng. Chem. Res.* **2008**, *47* (14), 4883−4890.
(16) Sevilla, M.; Valle-Vigón, P.; Fuertes, A. B. N-Doped polypyrrole-based porous carbons for CO_2 capture. *Adv. Funct. Mater.* **2011**, *21* (14), 2781−2787.
(17) Ma, X.; Cao, M.; Hu, C. Bifunctional HNO_3 catalytic synthesis of N-doped porous carbons for CO_2 capture. *J. Mater. Chem. A* **2013**, *1* (3), 913−918.
(18) Cheung, O.; Hedin, N. Zeolites and related sorbents with narrow pores for CO_2 separation from flue gas. *RSC Adv.* **2014**, *4* (28), 14480−14494.
(19) Trickett, C. A.; Helal, A.; Al-Maythalony, B. A.; Yamani, Z. H.; Cordova, K. E.; Yaghi, O. M. The chemistry of metal−organic frameworks for CO_2 capture, regeneration and conversion. *Nature Rev. Mater.* **2017**, *2*, 17045.
(20) Nguyen, P. T. K.; Nguyen, H. T. D.; Pham, H. Q.; Kim, J.; Cordova, K. E.; Furukawa, H. Synthesis and selective CO_2 capture properties of a series of hexatopic linker-based metal−organic frameworks. *Inorg. Chem.* **2015**, *54* (20), 10065−10072.
(21) Nguyen, N. T.; Furukawa, H.; Gandara, F.; Nguyen, H. T.; Cordova, K. E.; Yaghi, O. M. Selective capture of carbon dioxide under humid conditions by hydrophobic chabazite-type zeolitic imidazolate frameworks. *Angew. Chem., Int. Ed.* **2014**, *53* (40), 10645−10648.
(22) Wang, W.; Zhou, M.; Yuan, D. Carbon dioxide capture in amorphous porous organic polymers. *J. Mater. Chem. A* **2017**, *5* (4), 1334−1347.
(23) Zou, L.; Sun, Y.; Che, S.; Yang, X.; Wang, X.; Bosch, M.; Wang, Q.; Li, H.; Smith, M.; Yuan, S.; Perry, Z.; Zhou, H.-C. Porous organic polymers for post-combustion carbon capture. *Adv. Mater.* **2017**, *29* (37), 1700229.
(24) Zeng, Y.; Zou, R.; Zhao, Y. Covalent organic frameworks for CO_2 capture. *Adv. Mater.* **2016**, *28* (15), 2855−2873.
(25) Ma, Y.-X.; Li, Z.-J.; Wei, L.; Ding, S.-Y.; Zhang, Y.-B.; Wang, W. A dynamic three-dimensional covalent organic framework. *J. Am. Chem. Soc.* **2017**, *139* (14), 4995−4998.
(26) Dey, S.; Bhunia, A.; Esquivel, D.; Janiak, C. Covalent triazine-based frameworks (CTFs) from triptycene and fluorene motifs for CO_2 adsorption. *J. Mater. Chem. A* **2016**, *4* (17), 6259−6263.
(27) Hug, S.; Stegbauer, L.; Oh, H.; Hirscher, M.; Lotsch, B. V. Nitrogen-rich covalent triazine frameworks as high-performance platforms for selective carbon capture and storage. *Chem. Mater.* **2015**, *27* (23), 8001−8010.
(28) Díaz, U.; Corma, A. Ordered covalent organic frameworks, COFs and PAFs: From preparation to application. *Coord. Chem. Rev.* **2016**, *311*, 85−124.
(29) Luo, Y.; Li, B.; Wang, W.; Wu, K.; Tan, B. Hypercrosslinked aromatic heterocyclic microporous polymers: A new class of highly selective CO_2 capturing materials. *Adv. Mater.* **2012**, *24* (42), 5703−5707.
(30) Hu, L.; Ni, H.; Chen, X.; Wang, L.; Wei, Y.; Jiang, T.; Lü, Y.; Lu, X.; Ye, P. Hypercrosslinked polymers incorporated with imidazolium salts for enhancing CO_2 capture. *Polym. Eng. Sci.* **2016**, *56* (5), 573−582.
(31) Abdelnaby, M. M.; Alloush, A. M.; Qasem, N. A. A.; Al-Maythalony, B. A.; Mansour, R. B.; Cordova, K. E.; Al Hamouz, O. C. S. Carbon dioxide capture in the presence of water by an amine-based crosslinked porous polymer. *J. Mater. Chem. A* **2018**, *6* (15), 6455−6462.
(32) Dawson, R.; Adams, D. J.; Cooper, A. I. Chemical tuning of CO_2 sorption in robust nanoporous organic polymers. *Chem. Sci.* **2011**, *2* (6), 1173−1177.
(33) Chang, Z.; Zhang, D.-S.; Chen, Q.; Bu, X.-H. Microporous organic polymers for gas storage and separation applications. *Phys. Chem. Chem. Phys.* **2013**, *15* (15), 5430−5442.
(34) Ren, S.; Bojdys, M. J.; Dawson, R.; Laybourn, A.; Khimyak, Y. Z.; Adams, D. J.; Cooper, A. I. Porous, fluorescent, covalent triazine-based frameworks via room-temperature and microwave-assisted synthesis. *Adv. Mater.* **2012**, *24* (17), 2357−2361.
(35) Sun, L.-B.; Li, A.-G.; Liu, X.-D.; Liu, X.-Q.; Feng, D.; Lu, W.; Yuan, D.; Zhou, H.-C. Facile fabrication of cost-effective porous polymer networks for highly selective CO_2 capture. *J. Mater. Chem. A* **2015**, *3* (7), 3252−3256.
(36) Woodward, R. T.; Stevens, L. A.; Dawson, R.; Vijayaraghavan, M.; Hasell, T.; Silverwood, I. P.; Ewing, A. V.; Ratvijitvech, T.; Exley, J. D.; Chong, S. Y.; Blanc, F.; Adams, D. J.; Kazarian, S. G.; Snape, C. E.; Drage, T. C.; Cooper, A. I. Swellable, water- and acid-tolerant polymer sponges for chemoselective carbon dioxide capture. *J. Am. Chem. Soc.* **2014**, *136* (25), 9028−9035.
(37) Zhao, W.; Zhang, T.; Wang, Y.; Qiao, J.; Wang, Z. Corrosion failure mechanism of associated gas transmission pipeline. *Materials* **2018**, *11* (10), 1935.
(38) Dawson, R.; Stevens, L. A.; Drage, T. C.; Snape, C. E.; Smith, M. W.; Adams, D. J.; Cooper, A. I. Impact of water coadsorption for carbon dioxide capture in microporous polymer sorbents. *J. Am. Chem. Soc.* **2012**, *134* (26), 10741−10744.
(39) Hao, G.-P.; Li, W.-C.; Qian, D.; Wang, G.-H.; Zhang, W.-P.; Zhang, T.; Wang, A.-Q.; Schüth, F.; Bongard, H.-J.; Lu, A.-H. Structurally designed synthesis of mechanically stable poly(benzoxazine-co-resol)-based porous carbon monoliths and their application as high-performance CO_2 capture sorbents. *J. Am. Chem. Soc.* **2011**, *133* (29), 11378−11388.
(40) Kua, J.; Loli, H. Porphinogen formation from the co-oligomerization of formaldehyde and pyrrole: Free energy pathways. *J. Phys. Chem. A* **2017**, *121* (42), 8154−8165.
(41) Albakri, M. A.; Abdelnaby, M. M.; Saleh, T. A.; Al Hamouz, O. C. S. New series of benzene-1,3,5-triamine based cross-linked polyamines and polyamine/CNT composites for lead ion removal from aqueous solutions. *Chem. Eng. J.* **2018**, *333*, 76−84.
(42) Alcolea Palafox, M.; Gil, M.; Núñez, J. L.; Tardajos, G. Study of phenothiazine and N-methyl phenothiazine by infrared, raman, 1H-, and 13C-NMR spectroscopies. *Int. J. Quantum Chem.* **2002**, *89* (3), 147−171.
(43) Wang, S.; Zhang, C.; Shu, Y.; Jiang, S.; Xia, Q.; Chen, L.; Jin, S.; Hussain, I.; Cooper, A. I.; Tan, B. Layered microporous polymers by solvent knitting method. *Sci. Adv.* **2017**, *3* (3), No. e1602610.
(44) Weber, J.; Antonietti, M.; Thomas, A. Microporous networks of high-performance polymers: Elastic deformations and gas sorption properties. *Macromolecules* **2008**, *41* (8), 2880−2885.
(45) Sumida, K.; Rogow, D. L.; Mason, J. A.; McDonald, T. M.; Bloch, E. D.; Herm, Z. R.; Bae, T.-H.; Long, J. R. Carbon dioxide capture in metal−organic frameworks. *Chem. Rev.* **2012**, *112* (2), 724−781.
(46) Furukawa, H.; Yaghi, O. M. Storage of hydrogen, methane, and carbon dioxide in highly porous covalent organic frameworks for clean energy applications. *J. Am. Chem. Soc.* **2009**, *131* (25), 8875−8883.
(47) Mane, S.; Gao, Z.-Y.; Li, Y.-X.; Xue, D.-M.; Liu, X.-Q.; Sun, L.-B. Fabrication of microporous polymers for selective CO_2 capture: the significant role of crosslinking and crosslinker length. *J. Mater. Chem. A* **2017**, *5* (44), 23310−23318.
(48) Dawson, R.; Stöckel, E.; Holst, J. R.; Adams, D. J.; Cooper, A. I. Microporous organic polymers for carbon dioxide capture. *Energy Environ. Sci.* **2011**, *4* (10), 4239−4245.
(49) Lu, W.; Sculley, J. P.; Yuan, D.; Krishna, R.; Wei, Z.; Zhou, H.-C. Polyamine-tethered porous polymer networks for carbon dioxide capture from flue gas. *Angew. Chem., Int. Ed.* **2012**, *51* (30), 7480−7484.
(50) Nugent, P.; Belmabkhout, Y.; Burd, S. D.; Cairns, A. J.; Luebke, R.; Forrest, K.; Pham, T.; Ma, S.; Space, B.; Wojtas, L.; Eddaoudi, M.; Zaworotko, M. J. Porous materials with optimal adsorption thermodynamics and kinetics for CO_2 separation. *Nature* **2013**, *495*, 80−84.
(51) Bhunia, S.; Bhanja, P.; Das, S. K.; Sen, T.; Bhaumik, A. Triazine containing N-rich microporous organic polymers for CO_2 capture and

DOI: 10.1021/acssuschemeng.9b02334
ACS Sustainable Chem. Eng. 2019, 7, 13941−13948

unprecedented CO_2/N_2 selectivity. *J. Solid State Chem.* **2017**, *247*, 113−119.
(52) Patel, H. A.; Je, S. H.; Park, J.; Jung, Y.; Coskun, A.; Yavuz, C. T. Directing the structural features of N_2-phobic nanoporous covalent organic polymers for CO_2 capture and separation. *Chem. - Eur. J.* **2014**, *20* (3), 772−780.
(53) Ben, T.; Li, Y.; Zhu, L.; Zhang, D.; Cao, D.; Xiang, Z.; Yao, X.; Qiu, S. Selective adsorption of carbon dioxide by carbonized porous aromatic framework (PAF). *Energy Environ. Sci.* **2012**, *5* (8), 8370−8376.
(54) Wang, K.; Huang, H.; Liu, D.; Wang, C.; Li, J.; Zhong, C. Covalent triazine-based frameworks with ultramicropores and high nitrogen contents for highly selective CO_2 capture. *Environ. Sci. Technol.* **2016**, *50* (9), 4869−4876.
(55) Nguyen, N. T. T.; Lo, T. N. H.; Kim, J.; Nguyen, H. T. D.; Le, T. B.; Cordova, K. E.; Furukawa, H. Mixed-metal zeolitic imidazolate frameworks and their selective capture of wet carbon dioxide over methane. *Inorg. Chem.* **2016**, *55* (12), 6201−6207.
(56) Soubeyrand-Lenoir, E.; Vagner, C.; Yoon, J. W.; Bazin, P.; Ragon, F.; Hwang, Y. K.; Serre, C.; Chang, J.-S.; Llewellyn, P. L. How water fosters a remarkable 5-fold increase in low-pressure CO_2 uptake within mesoporous MIL-100(Fe). *J. Am. Chem. Soc.* **2012**, *134* (24), 10174−10181.
(57) Yu, J.; Zhai, Y.; Chuang, S. S. C. Water Enhancement in CO_2 capture by amines: An insight into CO_2−H_2O interactions on amine films and sorbents. *Ind. Eng. Chem. Res.* **2018**, *57* (11), 4052−4062.
(58) Mane, S.; Gao, Z.-Y.; Li, Y.-X.; Liu, X.-Q.; Sun, L.-B. Rational fabrication of polyethylenimine-linked microbeads for selective CO_2 capture. *Ind. Eng. Chem. Res.* **2018**, *57* (1), 250−258.
(59) Lu, W.; Verdegaal, W. M.; Yu, J.; Balbuena, P. B.; Jeong, H.-K.; Zhou, H.-C. Building multiple adsorption sites in porous polymer networks for carbon capture applications. *Energy Environ. Sci.* **2013**, *6* (12), 3559−3564.
(60) Huang, N.; Chen, X.; Krishna, R.; Jiang, D. Two-dimensional covalent organic frameworks for carbon dioxide capture through channel-wall functionalization. *Angew. Chem., Int. Ed.* **2015**, *54* (10), 2986−2990.
(61) Zhao, Y.; Yao, K. X.; Teng, B.; Zhang, T.; Han, Y. A perfluorinated covalent triazine-based framework for highly selective and water−tolerant CO_2 capture. *Energy Environ. Sci.* **2013**, *6* (12), 3684−3692.
(62) Yang, X.; Yu, M.; Zhao, Y.; Zhang, C.; Wang, X.; Jiang, J.-X. Hypercrosslinked microporous polymers based on carbazole for gas storage and separation. *RSC Adv.* **2014**, *4* (105), 61051−61055.
(63) Modak, A.; Nandi, M.; Mondal, J.; Bhaumik, A. Porphyrin based porous organic polymers: Novel synthetic strategy and exceptionally high CO_2 adsorption capacity. *Chem. Commun.* **2012**, *48* (2), 248−250.
(64) Modak, A.; Pramanik, M.; Inagaki, S.; Bhaumik, A. A triazine functionalized porous organic polymer: Excellent CO_2 storage material and support for designing Pd nanocatalyst for C−C cross-coupling reactions. *J. Mater. Chem. A* **2014**, *2* (30), 11642−11650.

DOI: 10.1021/acssuschemeng.9b02334
ACS Sustainable Chem. Eng. 2019, 7, 13941−13948